

Application of the pair torque interaction potential to simulate the elastic behavior of SLMoS₂

This content has been downloaded from IOPscience. Please scroll down to see the full text.

2016 Modelling Simul. Mater. Sci. Eng. 24 045003

(<http://iopscience.iop.org/0965-0393/24/4/045003>)

View [the table of contents for this issue](#), or go to the [journal homepage](#) for more

Download details:

IP Address: 195.209.230.53

This content was downloaded on 26/03/2016 at 14:23

Please note that [terms and conditions apply](#).

Application of the pair torque interaction potential to simulate the elastic behavior of SLMoS₂

I E Berinskii^{1,2}, A Yu Panchenko^{2,3} and E A Podolskaya^{2,3}

¹ School of Mechanical Engineering, Tel Aviv Univeristy, Ramat Aviv, Tel Aviv 69978, Israel

² Peter the Great St. Petersburg Polytechnic University, 29, Politechnicheskaya str., St. Petersburg, 195251, Russia

³ Institute for Problems in Mechanical Engineering RAS, 61, Bolshoy pr. V. O., St. Petersburg, 199178, Russia

E-mail: iberinsk@gmail.com

Received 27 August 2015, revised 20 February 2016

Accepted for publication 1 March 2016

Published 24 March 2016



CrossMark

Abstract

This paper is devoted to the application of the pair torque interaction potential for the simulation of the elastic behavior of a promising two-dimensional material: single layer molybdenum disulphide (SLMoS₂). It is demonstrated that both Mo–Mo and S–S interactions can be regarded as pair force interactions with sufficient accuracy. Using both experimental and calculated numerically elastic moduli, and also the phonon spectrum available in the literature, the parameters of the Morse potential are determined for Mo–Mo and S–S bonds, and the parameters of the pair torque potential are obtained for the Mo–S bond. As a result, a combination of force and torque pair potentials is proposed, which allows for the correct modelling of SLMoS₂ mechanical behavior.

Keywords: torque interaction, molybdenum disulfide, elasticity, MD simulation, two-dimensional materials

(Some figures may appear in colour only in the online journal)

1. Introduction

Two-dimensional (2D) (or quasi-two-dimensional) materials are relatively new materials having one dimension restricted. Graphene, a single layer of graphite, was the first 2D material obtained by mechanical exfoliation. Inspired by outstanding properties of graphene and its prospective scientific and technological impact, a lot of researchers were prompted to

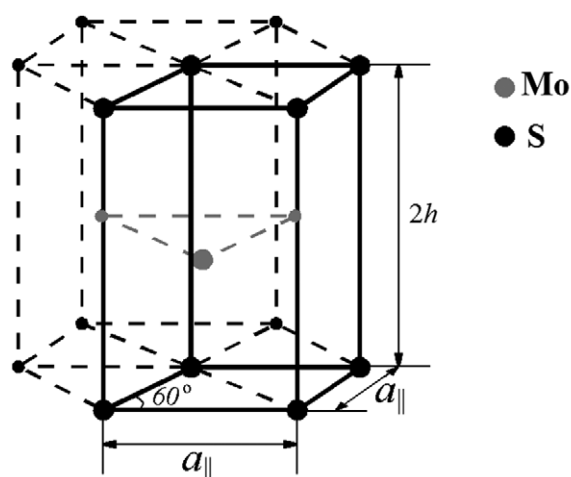


Figure 1. Unit cell of SLMoS₂ (solid lines). Grey circles are atoms of Mo, black circles are atoms of S.

produce other 2D materials. Nowadays, a wide variety of 2D metal oxides, hydroxides and chalcogenides, and metalorganic frameworks are obtained by physical and chemical methods including micromechanical cleavage, anodic bonding, chemical vapour deposition, molecular beam epitaxy, growth on the substrate, chemical synthesis, etc [1, 2]. These materials include hexagonal boron nitride, 2D honeycomb silicon, layered transition metal dichalcogenides (including MoS₂ and WS₂), black phosphorus, and 2D ZnO [3]. Unlike graphene, most 2D materials actually have several atomic layers. For example, single layered molybdenum disulphide (SLMoS₂) shown in figure 1, is part of a hexagonal close-packed (HCP) structure, which is infinite in the plane of transverse isotropy and has only three layers in the orthogonal direction. The top and bottom layers are occupied by sulfur (S) and the medium layer consists of molybdenum (Mo).

The complex lattice structure of SLMoS₂ in comparison with graphene's leads to its specific properties. Both these 2D materials are considered to be used for NEMS such as nanomechanical resonators in application to the ultra-precision mass sensing due to their large area and small thickness [4, 5]. Hence, it is crucial for them to be strong and elastic, and have a stable frequency of oscillations. The Young's modulus of SLMoS₂ is much smaller in comparison with that of graphene. However, its Q-factor (ability to preserve the oscillations) at room temperature is reported to be much higher as well as its bending rigidity [3]. Also, SLMoS₂ has another big advantage connected not with mechanical but electronic properties. Unlike graphene, which has an outstanding electrical conductivity, SLMoS₂ is a semiconductor with a direct band gap which makes it possible to use in single-layered nanoelectronic devices such as transistors [6] and memory cells [7].

This paper is devoted to the possible application of the pair torque interatomic potential for the modeling of the elastic behavior of SLMoS₂. Torque potentials are the generalized potentials of interaction that take into account torque interactions between the atoms in addition to the classical force interaction [8, 9]. It is well-known that pair force potentials such as Morse or Lennard-Jones potentials are hardly applicable to complex lattices, i.e. lattices having more than one atom in the unit cell. The reason is that the pair force interaction prescribes a certain symmetry of the bonds, which is typical only for simple lattices. Usually more complex approaches such as REBO or EAM potentials are used in molecular dynamics (MD)

Table 1. Lattice parameters of MoS₂.

Lattice parameters	SW potential [13]	DFT calculations [14]	Experiment [15]
$a_{\parallel}, \text{\AA}$	3.09	3.122	3.16
$a_{\perp}, \text{\AA}$	2.39	2.382	2.42

simulations for complex lattices. Due to the additional terms which stabilize a lattice, torque potentials also allow us to successfully describe the mechanics of complex lattices such as graphene [8, 10], a HCP lattice [11], diamond [12], etc. However, in contrast to the other potentials usually used in MD, torque interactions have a relatively simple form and their parameters possess clear physical meaning.

The paper is organized as follows. Section 2 is devoted to the construction of the SLMoS₂ stiffness tensor based on the microstructure of the crystal lattice, and only the bonds' stiffnesses are introduced. Section 3 introduces the pair torque potential for the Mo–S bond, and the simulation technique is described. Finally, in section 4 the stiffness tensor is revisited and also the phonon spectrum is plotted to identify the parameters of the interaction potentials for the bonds between Mo–S, Mo–Mo and S–S; afterwards, the bending modulus is calculated and compared with its values available in the literature. As a result, a combination of force and torque pair potentials is proposed, and it allows for the correct modeling of SLMoS₂ mechanical behavior.

2. Geometrical structure and stiffness tensor

This section is devoted to the construction of the stiffness tensor for SLMoS₂ and the consequent determination of the bonds' stiffnesses using the available experimental data on elastic moduli. The structure of SLMoS₂ is geometrically imperfect, as the distance a_{\perp} between Mo–S is smaller than a_{\parallel} between Mo–Mo and S–S. Each Mo has 12 neighboring atoms, i.e. six Mo in the plane of isotropy and six S above and beneath. The unit cell contains one Mo and two S. It consists of parallel rhombi lying in the S planes with the side a_{\parallel} and the angle of 60°, which are spaced at the distance $2h$, and Mo is located in the middle plane between the bases of the cell (see figure 1). The unit cell volume is

$$V_0 = \sqrt{3}ha_{\parallel}^2, \quad h = \sqrt{a_{\perp}^2 - \frac{a_{\parallel}^2}{3}}. \quad (1)$$

Table 1 shows the available data on lattice parameters from the parametrization of the Stillinger–Weber (SW) potential [13], first-principles calculations [14] and experiment [15].

Due to the geometrical imperfection of the lattice ($a_{\perp} \neq a_{\parallel}$) it is not actually close-packed, hence, pair force interaction potentials, which depend only on the distance between the atoms, are, in general, not applicable [11]. The approach proposed in this paper is the introduction of the pair torque potential, which results in the presence of not only longitudinal stiffness c_1 , but also shear stiffness c_2 of an interatomic bond [8]. Let us accept the nearest neighbor interaction hypothesis and take into account the fact that the material is infinite in the plane of transverse isotropy. Hence, we can use the theory for infinite crystals as the first approximation, i.e. not to account for boundary effects, and write down the macroscopic stiffness tensor of MoS₂ following [16] for a HCP lattice

$${}^4\mathbf{C} = {}^4\mathbf{C}_* - {}^3\mathbf{C} \cdot {}^2\mathbf{C}^{-1} \cdot {}^3\mathbf{C}, \quad (2)$$

where

$$\begin{aligned}
{}^2\mathbf{C} &= \frac{1}{V_0} \sum_{\alpha} \left[(c_1^{\text{MoS}} - c_2^{\text{MoS}}) \mathbf{n}_{\alpha} \mathbf{n}_{\alpha} + c_2^{\text{MoS}} \mathbf{I} \right] \\
{}^3\mathbf{C} &= \frac{a_{\perp}}{V_0} \sum_{\alpha} (c_1^{\text{MoS}} - c_2^{\text{MoS}}) \mathbf{n}_{\alpha} \mathbf{n}_{\alpha} \mathbf{n}_{\alpha} \\
{}^4\mathbf{C}_{*} &= \frac{a_{\perp}^2}{V_0} \sum_{\alpha} \left[(c_1^{\text{MoS}} - c_2^{\text{MoS}}) \mathbf{n}_{\alpha} \mathbf{n}_{\alpha} \mathbf{n}_{\alpha} \mathbf{n}_{\alpha} + c_2^{\text{MoS}} \mathbf{n}_{\alpha} \mathbf{I} \mathbf{n}_{\alpha} \right]^{\text{Sym}} \\
&\quad + \frac{a_{\parallel}^2}{2V_0} \sum_{\alpha} \left[(c_1^{\text{Mo}} - c_2^{\text{Mo}}) \mathbf{n}_{\alpha} \mathbf{n}_{\alpha} \mathbf{n}_{\alpha} \mathbf{n}_{\alpha} + c_2^{\text{Mo}} \mathbf{n}_{\alpha} \mathbf{I} \mathbf{n}_{\alpha} \right]^{\text{Sym}} \\
&\quad + \frac{a_{\parallel}^2}{V_0} \sum_{\alpha} \left[(c_1^{\text{S}} - c_2^{\text{S}}) \mathbf{n}_{\alpha} \mathbf{n}_{\alpha} \mathbf{n}_{\alpha} \mathbf{n}_{\alpha} + c_2^{\text{S}} \mathbf{n}_{\alpha} \mathbf{I} \mathbf{n}_{\alpha} \right]^{\text{Sym}} \quad (3)
\end{aligned}$$

The summation is carried out over the bonds which correspond to the upper indices of the stiffness coefficients c_1 and c_2 . The deformation of a complex lattice consists of the deformation of the sublattices (${}^4\mathbf{C}_{*}$), their displacement with respect to each other (${}^2\mathbf{C}$), and the mutual influence of these two types of deformations (${}^3\mathbf{C}$). The symmetrization sign ${}^{\text{Sym}}$ for the fourth-rank tensor means

$$({}^4C_{ijkl})^{\text{Sym}} = \frac{1}{4} (C_{ijkl} + C_{ijlk} + C_{jikl} + C_{jilk}) \quad (4)$$

The resulting stiffness tensor ${}^4\mathbf{C}$ is transversely isotropic, and it can be written in the following matrix form using Voigt notation

$$\begin{pmatrix}
C_{11} & C_{12} & C_{13} & 0 & 0 & 0 \\
C_{12} & C_{11} & C_{13} & 0 & 0 & 0 \\
C_{13} & C_{13} & C_{33} & 0 & 0 & 0 \\
0 & 0 & 0 & C_{44} & 0 & 0 \\
0 & 0 & 0 & 0 & C_{44} & 0 \\
0 & 0 & 0 & 0 & 0 & \frac{C_{11} - C_{12}}{2}
\end{pmatrix} \quad (5)$$

Thus, knowing the elastic moduli C_{ij} or their linear combinations, obtained either experimentally or from numerical simulation, we can determine the bonds' stiffnesses. Specifically, we minimize the function

$$\frac{|E_{xy} - E_{xy}^{\text{exp}}|}{E_{xy}^{\text{exp}}} + \frac{|\nu_{xy} - \nu_{xy}^{\text{exp}}|}{\nu_{xy}^{\text{exp}}} + \frac{|\nu_{xz} - \nu_{xz}^{\text{exp}}|}{\nu_{xz}^{\text{exp}}}, \quad (6)$$

where

$$\begin{aligned}
E_{xy} &= \frac{(C_{11} - C_{12})^2 C_{33} - 2(C_{11} - C_{12}) C_{13}^2}{C_{11} C_{33} - C_{13}^2} \\
\nu_{xy} &= \frac{C_{12} C_{33} - C_{13}^2}{C_{11} C_{33} - C_{13}^2}, \quad \nu_{xz} = \frac{C_{13}}{C_{11} + C_{12}}. \quad (7)
\end{aligned}$$

Here E_{xy} is Young's modulus in the plane of isotropy, ν_{xy} and ν_{xz} are in-plane and out-of-plane Poisson's ratios. Herewith, we demand that the stiffnesses are nonnegative and that the difference between the reference and the calculated moduli does not exceed 2%.

Table 2. Bonds' stiffnesses and elastic moduli of MoS₂.

Calculated bonds' stiffnesses (N m ⁻¹)	Calculated elastic moduli	Reference elastic moduli [17]
$c_1^{\text{Mo}} = 5.65$	$E_{xy} = 202 \text{ GPa}$	$E_{xy} = 200 \text{ GPa}$
$c_1^{\text{S}} = 10.29$	$\nu_{xy} = 0.2127$	$\nu_{xy} = 0.21$
$c_1^{\text{MoS}} = 74.85$	$\nu_{xz} = 0.2754$	$\nu_{xz} = 0.27$
$c_2^{\text{MoS}} = 17.72$		

Our calculations have shown that the torque components of Mo–Mo and S–S interactions are negligible. Hence, we further restrict ourselves purely to the force interaction between Mo–Mo and S–S, which can be considered the main result of this section. Table 2 shows the results of the calculations for micro- and macroscopic elastic parameters [15].

3. Pair torque potential and its application to simulations

3.1. Interaction potentials

In the previous section the stiffnesses of the interatomic bonds were determined, while the boundary effects were neglected. Let us now introduce the particular interaction laws, which will be further used for numerical simulation and more precise determination of elastic properties.

As for the Mo–Mo and S–S bonds, we use the Morse potential to model the respective force interactions

$$\begin{aligned}
 U_{\text{Mo}}(r) &= D_{\text{Mo}} \left[e^{2\theta_{\text{Mo}}\left(1-\frac{r}{a_{\text{Mo}}}\right)} - 2e^{\theta_{\text{Mo}}\left(1-\frac{r}{a_{\text{Mo}}}\right)} \right], \\
 U_{\text{S}}(r) &= D_{\text{S}} \left[e^{2\theta_{\text{S}}\left(1-\frac{r}{a_{\text{S}}}\right)} - 2e^{\theta_{\text{S}}\left(1-\frac{r}{a_{\text{S}}}\right)} \right].
 \end{aligned} \tag{8}$$

Here D_{Mo} and D_{S} are the depths of the respective potential wells, a_{Mo} and a_{S} are the equilibrium bond distances, θ_{Mo} and θ_{S} are responsible for the wells' widths. The respective longitudinal stiffnesses are

$$c_1^{\text{Mo}} = 2D_{\text{Mo}} \left(\frac{\theta_{\text{Mo}}}{a_{\text{Mo}}} \right)^2, \quad c_1^{\text{S}} = 2D_{\text{S}} \left(\frac{\theta_{\text{S}}}{a_{\text{S}}} \right)^2. \tag{9}$$

Let us turn to the torque interaction between Mo and S. Following [18, 19], let us consider two rigid particles with the indices i and j which interact via forces and torques. They, in turn, depend on the particles' relative position, relative orientation, and orientation with respect to the vector \mathbf{r}_{ij} which connects the particles, and the interactions are assumed to be potential. Thus, the internal energy U depends on \mathbf{r}_{ij} and on several unit vectors $\{\mathbf{n}_{ik}\}_{k \in \Lambda_i}$, rigidly connected with the particle, which describe the particles' orientation, where Λ_i is a set of indices.

Following the results of the previous section we use torque interaction to describe the elastic deformation of the Mo–S bond, and we restrict ourselves to the nearest neighbor interaction. Let us connect the particles with the bonds at the points which do not necessarily coincide with the particles' centers. For example, in the case shown in figure 2, the points lie on the particles' surfaces and R_i, R_j are the particles' radii. Let us introduce orthogonal unit vectors $\mathbf{n}_{i1}, \mathbf{n}_{i2}, \mathbf{n}_{i3}$ and $\mathbf{n}_{j1}, \mathbf{n}_{j2}, \mathbf{n}_{j3}$, where the first indices correspond to the particles' numbers, and

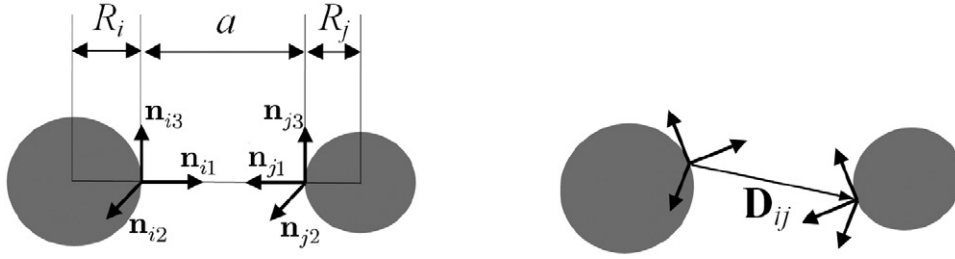


Figure 2. Two bonded particles in undeformed (left) and deformed (right) states [18].

the second indices correspond to the vectors' numbers. In the undeformed state the following relations are satisfied

$$\mathbf{n}_{i1} = -\mathbf{n}_{j1} = \frac{\mathbf{r}_{ij}}{r_{ij}}, \quad \mathbf{n}_{i2} = \mathbf{n}_{j2}, \quad \mathbf{n}_{i3} = \mathbf{n}_{j3}. \quad (10)$$

Let us neglect the bending and torsion bond stiffnesses [18], and thus restrict ourselves to longitudinal and shear ones. Then, the potential energy of the Mo–S bond is considered to have the following form

$$U_{\text{MoS}} = \frac{c_1}{2}(D_{ij} - a)^2 + \frac{c_2 a^2}{2}(\mathbf{n}_{j1} - \mathbf{n}_{i1}) \cdot \mathbf{d}_{ij}, \quad \mathbf{d}_{ij} = \frac{\mathbf{D}_{ij}}{D_{ij}}. \quad (11)$$

Here i and j can be referred to as Mo and S. The upper indices MoS of the stiffnesses c_1 and c_2 are further omitted. Vector $\mathbf{D}_{ij} = \mathbf{r}_i + R_i \mathbf{n}_{i1} - R_j \mathbf{n}_{j1} - R_i \mathbf{n}_{i1}$ connects the ends of the bond with radius vectors $\mathbf{r}_i + R_i \mathbf{n}_{i1}$, $\mathbf{r}_j + R_j \mathbf{n}_{j1}$, and $a = a_{\perp} - R_i - R_j$ (see figure 2). The force \mathbf{F}_{ij} and torque \mathbf{M}_{ij} can be calculated as

$$\begin{aligned} \mathbf{F}_{ij} &= -\mathbf{F}_{ji} = \frac{\partial U_{\text{MoS}}}{\partial \mathbf{r}_{ij}} = c_1(D_{ij} - a)\mathbf{d}_{ij} + \frac{c_2 a^2}{2D_{ij}}(\mathbf{n}_{j1} - \mathbf{n}_{i1}) \cdot (\mathbf{I} - \mathbf{d}_{ij}\mathbf{d}_{ij}), \\ \mathbf{M}_{ij} &= \sum_{k \in \Lambda_i} \frac{\partial U_{\text{MoS}}}{\partial \mathbf{n}_{ik}} \times \mathbf{n}_{ik} = R_i \mathbf{n}_{i1} \times \mathbf{F}_{ij} - \frac{c_2 a^2}{2} \mathbf{d}_{ij} \times \mathbf{n}_{i1}, \\ \mathbf{M}_{ji} &= \sum_{m \in \Lambda_j} \frac{\partial U_{\text{MoS}}}{\partial \mathbf{n}_{jm}} \times \mathbf{n}_{jm} = R_j \mathbf{n}_{j1} \times \mathbf{F}_{ji} + \frac{c_2 a^2}{2} \mathbf{d}_{ij} \times \mathbf{n}_{j1}. \end{aligned} \quad (12)$$

In addition to the parameters c_1 and c_2 , we need to determine the radii R_{Mo} and R_{S} , and also the particles' masses and moments of inertia, which in general are not directly related to the masses.

3.2. Simulation technique

The particle dynamics method is used for the simulations. The main idea of the method is close to the discrete [20] and distinct [21] element methods and other generalizations of classical MD. In this work, particles are simulated as the rigid bodies. The masses of the bodies are equal to the real masses of the interacting atoms. The moments of inertia are calculated as if the particles were balls ($2mR^2/5$), and inertia tensor is spherical, without loss of generality.

The position of the center of mass of any particle in any layer is determined by the solution of the following equation of motion

$$m_j \ddot{\mathbf{u}}_j = \sum_{i \neq j} -\frac{\partial U}{\partial \mathbf{r}_{ij}}, \quad (13)$$

where

$$U = \begin{cases} U_{\text{MoS}} + U_{\text{Mo}}, & j \in \text{Mo} \\ U_{\text{MoS}} + U_{\text{S}}, & j \in \text{S} \end{cases} \quad (14)$$

The rotation of the particles is described as

$$\Theta_j(\omega_j \mathbf{w}_j) = \sum_{i \neq j} \mathbf{M}_{ij}, \quad (15)$$

where Θ_j is a moment of inertia, ω_j is an angular velocity. A unit vector \mathbf{w}_j determines the axis of rotation at the current time step. Its components can be found from the integration of equation (15).

The quaternions formalism [22] is applied to calculate new orientation vectors \mathbf{n}_{jk} for any particle, where $k = 1, 2, 3$ and j is a particle index (figure 2). Rotation around the vector \mathbf{w}_j is calculated at each time step dt using quaternions \mathbf{q}_j :

$$\begin{aligned} \mathbf{q}_j(t + dt) &= \mathbf{q}_j(t) * d\mathbf{q}_j, \\ d\mathbf{q}_j &= \cos\left(\frac{\omega_j dt}{2}\right) + \mathbf{w}_j \sin\left(\frac{\omega_j dt}{2}\right). \end{aligned} \quad (16)$$

Vectors \mathbf{n}_{jk} are given by the following relation

$$\mathbf{n}_{jk}(t + dt) = \mathbf{q}_j * \mathbf{n}_{jk}(t) * \mathbf{q}_j^{-1}. \quad (17)$$

The equations (13) and (15) are integrated at each step using a leap-frog algorithm [23].

4. Parameter determination

In this section we determine the parameters of the interatomic potentials (8) and (11). We calculate the elastic moduli and the phonon spectrum, and try to find the parameters to match the reference values shown in table 2 and the reference spectrum. Afterwards, we obtain the out-of-plane bending modulus and compare its value with the results reported in the literature.

4.1. Stiffness tensor

We construct a mathematical model of SLMoS₂ using the method of molecular mechanics. The boundary effects in the plane of isotropy are eliminated by the introduction of periodic boundary conditions, whereas the upper and lower boundaries are free. Due to the nearest neighbor interaction assumption, the equilibrium state is stress-free. Hence, in order to determine the components of the stiffness tensor we need to solve a set of problems in which the material is subject to a homogeneous strain field with one non-zero component. We write the Hooke's law in the form

$$\frac{\Delta \sigma_{kl}}{\Delta \varepsilon_{ij}} = \frac{1}{2}(C_{kl ij} + C_{kl ji}), \quad i, j, k, l = 1, 2, 3, \quad (18)$$

where ε_{ij} and σ_{kl} are the components of strain and Cauchy stress tensors respectively, and $C_{kl ij}$ are the components of the stiffness tensor. The problems are solved using central differences

for $\varepsilon_{ij} = \pm 10^{-5}$, and consequently $\Delta\varepsilon_{ij} = 2 \cdot 10^{-5}$. Note, that the lattice of SLMoS₂ is complex, thus, it is also necessary to calculate the infinitesimal sublattice shift for each deformation so as to maintain the equilibrium. The non-zero components of the stiffness tensor are determined by the appearance of the non-zero components of the stress tensor as a result of the imposed strain, and the stress tensor is calculated as

$$\sigma = \frac{1}{2V_0} \sum_{\alpha} \mathbf{a}_{\alpha} \mathbf{F}_{\alpha}, \quad (19)$$

where the summation is carried out over all bond vectors \mathbf{a}_{α} . This method allows us to obtain only the part of the stiffness tensor which is symmetrical with respect to the permutation of the second pair of indices. Moreover, it turned out to be symmetrical with respect to the permutation of the first pair of indices as well, which allows us to use Voigt notation. Consequently, the stiffness tensor has the form (5).

4.2. Phonon spectrum

Note that the Mo–S interaction is determined by six parameters. These bonds lie out of the isotropy plane, but we possess the data on only three elastic moduli, besides the only available out-of-plane macroscopic elastic parameter is ν_{xz} , which is definitely not enough. In order to overcome this obstacle, let us construct the phonon spectrum. The spectrum of SLMoS₂ contains three acoustic and six optical branches. Both experimental and numerically calculated spectra along the main directions in the first Brillouin zone for SLMoS₂ are available in e.g. [24, 17, 13].

Let us substitute the following particles' displacements in the equations of motion

$$\begin{aligned} m \frac{d^2 \mathbf{u}_j}{dt^2} &= - \frac{\partial U}{\partial \mathbf{u}_j} \\ \mathbf{u}_j(\mathbf{r}, t) &= \mathbf{u}_{0j} e^{i\mathbf{k} \cdot \mathbf{r}} e^{-i\omega t}, \end{aligned} \quad (20)$$

where indices $j = 1, 2, 3$ correspond to medium, top and bottom layers of SLMoS₂, occupied by Mo, S and S respectively, \mathbf{k} is wave vector, i is an imaginary unit. Further, following [25], let us construct the dynamical matrix

$$\mathbf{Q}(\mathbf{k}) = \sum_{\mathbf{r}} \mathbf{Q}(\mathbf{r}) e^{-i\mathbf{k} \cdot \mathbf{r}}, \quad \mathbf{Q}(\mathbf{r}) = \frac{\partial^2 U}{\partial \mathbf{r}^2}. \quad (21)$$

The summation is carried out over the nearest neighbors.

The dynamical matrix for the Morse potential is

$$\mathbf{Q}(\mathbf{r}) = \left[U'' - \frac{U'}{r} \right] \mathbf{r}\mathbf{r} + \frac{U'}{r} \mathbf{I}, \quad (22)$$

whereas for the torque potential it has the form

$$\begin{aligned} \mathbf{Q}_{\text{MoS}}(\mathbf{r}) &= \left[\frac{c_1}{D_{ij}} (D_{ij} - a) - \frac{c_2 a^2}{2D_{ij}^3} (\mathbf{n}_{j1} - \mathbf{n}_{i1}) \cdot \mathbf{D}_{ij} \right] \mathbf{I} \\ &\quad - \frac{c_2 a^2}{2D_{ij}^3} [\mathbf{D}_{ij} (\mathbf{n}_{j1} - \mathbf{n}_{i1}) + (\mathbf{n}_{j1} - \mathbf{n}_{i1}) \mathbf{D}_{ij}] \\ &\quad + \left[\frac{c_1 a}{D_{ij}^3} + \frac{3c_2 a^2}{2D_{ij}^5} (\mathbf{n}_{j1} - \mathbf{n}_{i1}) \cdot \mathbf{D}_{ij} \right] \mathbf{D}_{ij} \mathbf{D}_{ij}. \end{aligned} \quad (23)$$

Finally, the equations of motion can be written as

$$\begin{aligned}
-\mathbf{u}_{01}m_{\text{Mo}}\omega^2 &= \mathbf{u}_{01} \sum_{\text{Mo}} \mathbf{Q}_{\text{Mo}}(\mathbf{r}) [e^{i\mathbf{k}\cdot\mathbf{r}} - 1] \\
&\quad + \sum_{\text{S(top)}} \mathbf{Q}_{\text{MoS}}(\mathbf{r}) [\mathbf{u}_{02}e^{i\mathbf{k}\cdot\mathbf{r}} - \mathbf{u}_{01}] \\
&\quad + \sum_{\text{S(bottom)}} \mathbf{Q}_{\text{MoS}}(\mathbf{r}) [\mathbf{u}_{03}e^{i\mathbf{k}\cdot\mathbf{r}} - \mathbf{u}_{01}] \\
-\mathbf{u}_{02}m_{\text{S}}\omega^2 &= \mathbf{u}_{02} \sum_{\text{S(top)}} \mathbf{Q}_{\text{S}}(\mathbf{r}) [e^{i\mathbf{k}\cdot\mathbf{r}} - 1] \\
&\quad + \sum_{\text{S(top)}} \mathbf{Q}_{\text{MoS}}(\mathbf{r}) [\mathbf{u}_{01}e^{i\mathbf{k}\cdot\mathbf{r}} - \mathbf{u}_{02}] \\
-\mathbf{u}_{03}m_{\text{S}}\omega^2 &= \mathbf{u}_{03} \sum_{\text{S(bottom)}} \mathbf{Q}_{\text{S}}(\mathbf{r}) [e^{i\mathbf{k}\cdot\mathbf{r}} - 1] \\
&\quad + \sum_{\text{S(bottom)}} \mathbf{Q}_{\text{MoS}}(\mathbf{r}) [\mathbf{u}_{01}e^{i\mathbf{k}\cdot\mathbf{r}} - \mathbf{u}_{03}]
\end{aligned} \tag{24}$$

The solution of this system yields to the eigenvalue problem for 9×9 symmetric matrix $\mathbf{Q}_{\text{Sum}}(\mathbf{k})$, which consists of $\mathbf{Q}_{\text{Mo}}(\mathbf{r})$, $\mathbf{Q}_{\text{MoS}}(\mathbf{r})$ and $\mathbf{Q}_{\text{S}}(\mathbf{r})$. Solving the equation

$$\det [\mathbf{Q}_{\text{Sum}}(\mathbf{k}) - \omega^2 \mathbf{I}_{9 \times 9}] = 0, \tag{25}$$

we get nine values of ω^2 , which correspond to the given wave vector \mathbf{k} , and, thus, the whole phonon spectrum.

Finally, the following fitting procedure is carried out to match the calculated and experimental elastic moduli, and to provide sufficient accuracy for the phonon spectrum curves. We determine the derivatives of the elastic moduli E_{xy} , ν_{xy} , ν_{xz} over the potentials' parameters and use the gradient descent method to search the minimal standard deviation from the experimental points [24] in the phonon spectrum. Herewith, we tried to provide an adequate deviation of the calculated elastic moduli values from the reference ones, and the results of the section 2 were used as a starting point. The results of the calculations are shown in figure 3 and table 3. The additional analysis has shown that the presence of bending and torsion bond stiffnesses does not influence the result, and their values cannot be determined from the elastic moduli and phonon spectrum.

The majority of the refined values of bond stiffnesses have the same order of magnitude as the ones obtained in section 2 (see table 2). The most significant difference is observed for the shear stiffness of the Mo–S bond, connected with the introduction of the particles' radii. Namely, the definition of the parameter which is responsible for interparticle distance is changed in comparison to section 2.

4.3. Bending modulus

Let us now calculate the out-of-plane bending modulus using the obtained potential parameters. Let us use a classical expression for the bending stiffness of the isotropic plate as a rough approximation:

$$B_{\text{shell}} = \frac{E_{xy}(2h)^3}{12(1 - \nu_{xy}^2)}. \tag{26}$$

This relation gives the value of 3.67 eV for our parameters. Here we assume that the thickness is equal to the height of the unit cell (see figure 1). The same formula was used in [26], and the

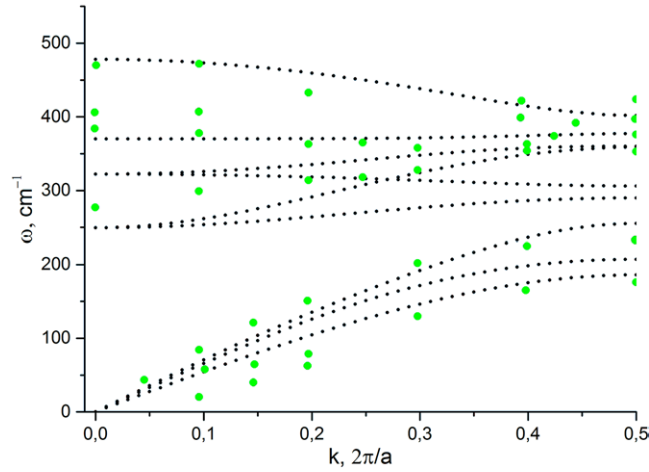


Figure 3. Phonon spectrum along ΓM direction in the first Brillouin zone for SLMoS₂: experimental data [24] (green dots) and calculation results (black dotted lines).

Table 3. The parameters of the interaction potentials for SLMoS₂ and calculated elastic moduli.

Elastic moduli	Value	Deviation					
E_{xy} , GPa	206	3.0% [17]					
ν_{xy}	0.245	16.7% [17]					
ν_{xz}	0.277	2.6% [17]					
B , eV	40.92	325.8% [26]					
c_1 , N m ⁻¹	c_2 , N m ⁻¹	R_{Mo} , Å	R_S , Å	D_{Mo} , eV	D_S , eV	θ_{Mo}	θ_S
97.4	738.2	1.08	0.8	$1.42 \cdot 10^{-2}$	$4.97 \cdot 10^{-2}$	12.32	11.11

obtained bending modulus lies between 6.62 eV and 13.24 eV with the same assumption on thickness. The difference between the obtained $B_{shell} = 3.67$ eV and the corridor, determined in [26], is explained by the different sources of experimental in-plane data.

However, it is known that shell theory might give inadequate results for nanosized structures [27], due to the ambiguous definition of thickness. Another approach, that does not account for thickness, is to calculate strain energy density W , which is assumed to have the following form

$$W = \frac{1}{2} B \kappa^2, \quad (27)$$

where κ is curvature, and B is the bending modulus. This approximation can be considered reasonable if infinitesimal strain is regarded. We carry out a quasistatic numerical simulation of cylindrical bending, and the bending radius is two orders of magnitude larger than the linear dimension of the sample. Strain energy density W is determined as the ratio of the total potential energy of the sample and its area, and the calculated value of the bending modulus is 40.92 eV (see table 3). This result differs significantly from the value of 9.61 eV reported in [26] as a result of bending simulation for the SW potential. It is important to remember that SLMoS₂ consists of three layers, and the presence of out-of-plane bonds results in the increase of the out-of-plane rigidity. So, the main contribution to the bending modulus is made by the

MoS bond, specifically, its shear stiffness c_2 . The obtained value of the bending modulus, which is rather high in comparison with B_{shell} , is a consequence of high out-of-plane bond stiffnesses, and SLMoS₂ cannot be described within thin shell theory. In turn, the difference of the obtained value and the value reported in [26] is caused by the contribution of the torque interaction.

5. Conclusions

We studied the possible application of the pair torque interaction potential [18] to the modeling of the elastic behavior of SLMoS₂. First, the approximate values of interatomic bonds' stiffnesses were obtained for infinite crystal, and we have demonstrated that both Mo–Mo and S–S interactions can be regarded as pair force interactions with sufficient accuracy. Then, the interaction laws were introduced. Based on both experimental and calculated numerically elastic moduli, and the phonon spectrum available in the literature, the parameters of the Morse potential were determined for both types of interaction, and the parameters of the torque potential were obtained for the Mo–S bond. The verification of the model is done by calculation of the bending modulus. On the whole, a good agreement is observed between the proposed model and both the experimental and numerical data on the elastic moduli and phonon spectrum.

The main result of this work is the proposed combination of force and torque pair potentials which can be further used for numerical simulation of various experiments on MoS₂.

Acknowledgments

This work was supported by the Russian Foundation for Basic Research (Grant No. 14-01-31487 mol_a) and by the President of the Russian Federation (Grant No. MK-4873.2014.1). The authors are deeply grateful to Prof A M Krivtsov, Dr V A Kuzkin and Dr M B Babenkov for fruitful discussions.

References

- [1] Mas-Balleste R, Gomez-Navarro C, Gomez-Herrero J and Zamora F 2011 2D materials: to graphene and beyond *Nanoscale* **3** 20–30
- [2] Bonaccorso F, Lombardo A, Hasan T, Sun Z, Colombo L and Ferrari A C 2012 Production and processing of graphene and 2D crystals *Mater. Today* **15** 564–89
- [3] Jiang J-W 2015 Graphene versus MoS₂: a short review *Front. Phys.* **10** 287–302
- [4] Chen C and Hone J 2013 Graphene nanoelectromechanical systems *Proc. IEEE* **101** 1766–79
- [5] Lee J, Wang Z, He K, Shan J and Feng P X-L 2013 High frequency MoS₂ nanomechanical resonators *ACS Nano* **7** 6086–91
- [6] Radisavljevic B, Radenovic A, Brivio J, Giacometti V and Kis A 2011 Single-layer MoS₂ transistors *Nat. Nanotechnol.* **6** 147–50
- [7] Bertolazzi S, Krasnozhan D and Kis A 2013 Nonvolatile memory cells based on MoS₂/graphene heterostructures *ACS Nano* **7** 3246–52
- [8] Ivanova E A, Krivtsov A M and Morozov N F 2007 Derivation of macroscopic relations of the elasticity of complex crystal lattices taking into account the moment interactions at the microlevel *J. Appl. Math. Mech.* **71** 543–61
- [9] Grekova E and Maugin G 2005 Modelling of complex elastic crystals by means of multi-spin micromorphic media *Int. J. Eng. Sci.* **43** 494–519
- [10] Berinskii I E, Ivanova E A, Krivtsov A M and Morozov N F 2007 Application of moment interaction to the construction of a stable model of graphite crystal lattice *Mech. Solids* **42** 663–71

- [11] Podolskaya E A and Krivtsov A M 2012 Description of the geometry of crystals with a hexagonal close-packed structure based on pair interaction potentials *Phys. Solid State* **54** 1408–16
- [12] Krivtsov A M and Loboda O S 2012 Description of elastic properties of diamond- and sphalerite-structured diatomic crystals with the use of moment interaction *Phys. Mesomech.* **15** 238–44
- [13] Jiang J-W, Park H S and Rabczuk T 2013 Molecular dynamics simulations of single-layer molybdenum disulphide (MoS₂): Stillinger-weber parametrization, mechanical properties and thermal conductivity *J. Appl. Phys.* **114** 064307
- [14] Cooper R C, Lee C, Marianetti C A, Wei X, Hone J and Kysar J W 2013 Nonlinear elastic behavior of two-dimensional molybdenum disulfide *Phys. Rev. B* **87** 035423
- [15] Böker Th, Severin R, Müller A, Janowitz C, Manzke R, Voß D, Krüger P, Mazur A and Pollmann J 2001 Band structure of MoS₂, MoSe₂ and α -MoTe₂: angle-resolved photoelectron spectroscopy and *ab initio* calculations *Phys. Rev. B* **64** 235305
- [16] Krivtsov A M and Podolskaya E A 2010 Modeling of elastic properties of crystals with hexagonal close-packed lattice *Mech. Solids* **45** 370–8
- [17] Tianshu Li 2012 Ideal strength and phonon instability in single-layer MoS₂ *Phys. Rev. B* **85** 235407
- [18] Kuzkin V A and Asonov I E 2012 Vector-based model of elastic bonds for simulation of granular solids *Phys. Rev. E* **86** 051301
- [19] Kuzkin V A 2015 Addendum to ‘Vector-based model of elastic bonds for simulation of granular solids’ arXiv:1507.06957
- [20] Cundall P A and Strack O D L 1979 A discrete numerical model for granular assemblies *Geotechnique* **29** 47–65
- [21] Ostanin I, Ballarini R, Potyondy D and Dumitrică T 2013 A distinct element method for large scale simulations of carbon nanotube assemblies *J. Mech. Phys. Solids* **61** 762–82
- [22] Altmann S L 1986 *Rotations, Quaternions and Double Groups* (Oxford: Clarendon)
- [23] Allen M P and Tildesley D J 1989 *Computer Simulation of Liquids* (Oxford: Oxford University Press)
- [24] Wakabayashi N, Smith H G and Nicklow R M 1975 Lattice dynamics of hexagonal MoS₂ studied by neutron scattering *Phys. Rev. B* **12** 659–63
- [25] Ashcroft N W and Mermin N D 1976 *Solid State Physics* (Philadelphia, PA: Saunders)
- [26] Jiang J-W, Qi Z, Park H S and Rabczuk T 2013 Elastic bending modulus of single-layer molybdenum disulfide (MoS₂): finite thickness effect *Nanotechnology* **24** 435705
- [27] Berinskii I E, Krivtsov A M and Kudarova A M 2014 Bending stiffness of a graphene sheet *Phys. Mesomech.* **17** 356–64